Bioconjugate Chemistry

Article

Design, synthesis, conjugation and reactivity of novel trans,trans-1,5-cyclooctadiene-derived bioorthogonal linkers

Beatrice Longo, Chiara Zanato, Monica Piras, Sergio Dall'Angelo, Albert D Windhorst, Danielle Vugts, Massimiliano Baldassarre, and Matteo Zanda

Bioconjugate Chem., **Just Accepted Manuscript** • DOI: 10.1021/acs.bioconjchem.0c00375 • Publication Date (Web): 30 Jul 2020

Just Accepted

is published by the American Chemical Society. 1155 Sixteenth Street N.W., Washington, DC 20036

Design, synthesis, conjugation and reactivity of novel *trans,trans*-1,5-cyclooctadiene-derived bioorthogonal linkers

Beatrice Longo,[a,b] Chiara Zanato,[a] Monica Piras,[a] Sergio Dall'Angelo,[a] Albert D. Windhorst,[c] Danielle J. Vugts,[c,*] Massimiliano Baldassarre,[a,*] Matteo Zanda[a,b,d,*]

[a]Institute of Medical Sciences, Foresterhill, University of Aberdeen, AB252ZD Aberdeen (UK)
[b]Centre for Sensing and Imaging Science, School of Science, Loughborough University, LB11 3TU Loughborough (UK)
[c]Amsterdam UMC, Vrije Universiteit, dept. Radiology and Nuclear Medicine, De Boelelaan 1117, 1081 HV Amsterdam, The Netherlands
[d]CNR-SCITEC, via Mancinelli 7, 20131 Milan (Italy)

ABSTRACT: The tetrazine/*trans* cyclooctene (TCO) inverse-electron-demand Diels-Alder (IEDDA) reaction is the fastest bioorthogonal "click" ligation process reported to date. In this context, TCO reagents have found widespread applications, however their availability and structural diversity is still somewhat limited, due to challenges connected with their synthesis and structural modification. To address this issue, we developed a novel strategy for the conjugation of TCO derivatives to a biomolecule, which allows for the creation of greater structural diversity from a single precursor molecule, i.e. *trans,trans*-1,5-cyclooctadiene [(*E*,*E*)-COD] **1**, whose preparation requires standard laboratory equipment and readily available reagents. This two-step strategy relies on the use of new bifunctional TCO-linkers (**5a-11a**) for IEDDA reactions, which can be synthesized *via* 1,3-dipolar cycloaddition of (*E*,*E*)-COD **1** with different azido-spacers (**5-11**) carrying an electrophilic function (NHS-ester, *N*-succinimidyl carbonate, *p*-nitrophenyl-carbonate, maleimide) in the ω-position. Following bioconjugation of these electrophilic linkers to the nucleophilic residue (cysteine or lysine) of a protein (step 1), the resulting TCO-decorated constructs can be subjected to a IEDDA reaction with tetrazines functionalized with fluorescent or near infrared (NIR) tags (step 2). We successfully used this strategy to label bovine serum albumin with the TCO-linker **8a** and subsequently reacted it in a cell lysate with the fluorescein-isothiocyanate (FITC)-derived tetrazine **12**. The same strategy was then used to label the bacterial wall of gram-positive *S. aureus* showing the potential of these linkers for live-cell imaging. Finally, we determined the impact of structural differences of the linkers upon the stability of the bioorthogonal constructs. The compounds for stability studies were prepared by conjugation of TCO-linkers **6a**, **8a** and **10a** to mAbs, such as Rituximab and Obinutuzumab, and subsequent labelling with a reactive Cy3-functionalized tetrazine.

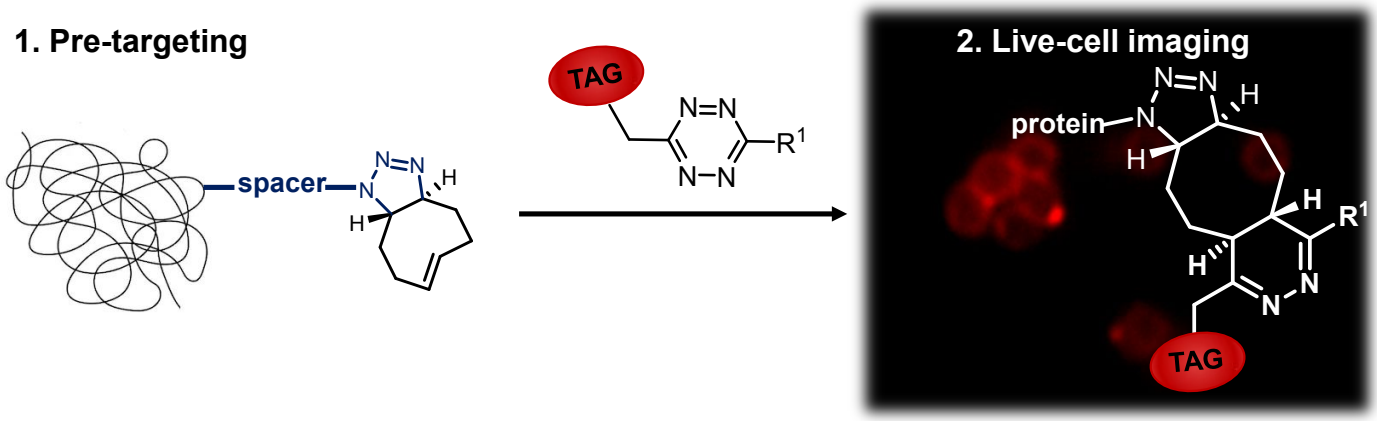

TOC GRAPHIC

INTRODUCTION

Reactions that proceed efficiently in biological systems are witnessing widespread applications in the fields of chemistry, chemical biology, material sciences and molecular diagnostics, where they enable manipulation of biomolecules, cells and particles and their tracking *in vitro* and *in vivo.*[1] Pioneered by Bertozzi's Staudinger ligation,[2] several bioorthogonal reactions were subsequently designed and developed. These reactions include the strain-promoted azide-alkyne cycloaddition (SPAAC) and the inverse electron-demand Diels-Alder (IEDDA) reaction.[3] In particular, the IEDDA reaction between 1,2,4,5-tetrazines and unsaturated compounds, sometimes referred to as Carboni-Lindsey[4] reaction, has attracted increasing attention in the last decade. In 1990, Sauer described the remarkable kinetics of electron-deficient tetrazines reacting with different olefins, reporting *trans*-cyclooctene (TCO) as the most reactive dienophile.[5] In 2008, two groups[6,7] almost simultaneously recognised the great potential of the tetrazine/TCO ligation, setting the stage for the development of a powerful bioorthogonal reaction.[8] Being the fastest click reaction reported to date, this process is a powerful tool for studying protein function and dynamics,[9,10] through incorporation of TCO reporters *via* chemical,[11] genetic[12] or enzymatic[13] methods. The TCO/tetrazine reaction proved its usefulness also in the radiochemistry field,[14] where it enabled the generation of modular radioligands in high radiochemical yields and specific activity.[15–17] In pre-clinical setting, the pre-targeted imaging of living mice[18–21] was pioneered by the group of Robillard.[22] Only the IEDDA reaction – among all the bioorthogonal ligations – has so far shown potential for *in vivo* applications, because reactant pairs must display high stability, selectivity and fast reactivity for *in vivo* applications.[18] Several papers were published in the last few years describing TCO derivatives with improved reactivity, stability and solubility.[23] (*E*)-Cyclooct-4-enol is a key TCO derivative which has been conjugated to biomolecules, typically antibodies, *via* functionalization with electrophilic linkers – such as succinimidyl esters and maleimides – reacting with nucleophilic lysine or cysteine residues of the biomolecule.[22,24,25] Fox and co-workers reported the extremely fast IEDDA kinetics of (*E*)-bicyclo[6.1.0]non-4-ene, due to the 8-membered ring being forced in a half-chair conformation (Fig. 1).[26] However, enhanced reactivity is often gained at the expense of stability. To overcome this problem, the same research group developed another conformationally-strained TCO, the *cis*-dioxolane-fused *trans*-cyclooctene (Fig. 1), which displayed enhanced stability, while maintaining high reactivity.[27] Recently, Lambert et al. reported the smaller and hydrophilic *trans*-5-oxocene,[28] following the work of the Kele group, who demonstrated that the lower lipophilicity of a dioxo-TCO derivative resulted in improved washout times during imaging experiments.[29] Despite these remarkable improvements and diverse applications of TCO linkers, their accessibility and commercial availability is still limited,[18] which could be partly ascribed to the persisting challenges connected with their synthesis and structural modification.[30] In this work, we aimed to develop a new portfolio of TCO-linkers that could be used for biorthogonal ligations, exploiting the capacity of *trans,trans*-1,5-cyclooctadiene [(*E*,*E*)-COD] **1** to undergo a double 'click' reaction. Highly strained (*E*,*E*)-COD **1** was first synthesized in 1958 by Wittig and Polster,[31] but it was not until 2011 that the Leeper group studied its unique reactivity, elegantly describing the capacity of **1** to undergo two successive click reactions:[32] one *trans*-double bond could be used for the conjugation to the target biomolecule, while the other was retained for the subsequent IEDDA bioorthogonal reaction with tetrazines. With this concept in mind, we synthesised a set of *trans*-triazoline-fused *trans*-cyclooctene linkers **5a-11a** (Fig. 1) *via* 1,3-dipolar cycloaddition of (*E*,*E*)-COD **1** with different azido-spacers **5-11** carrying an electrophilic function. Following bioconjugation of these electrophilic linkers to the nucleophilic residue (cysteine or lysine) of a protein (step 1), the resulting TCO-decorated constructs were subjected to IEDDA reaction with tetrazines functionalized with a fluorescent dye (step 2). The usefulness of these novel linkers as bioorthogonal reporters was demonstrated by the successful labelling of a protein (bovine serum albumin, BSA), bacteria (*Staphylococcus aureus*) and two therapeutic monoclonal antibodies (Rituximab and Obinutuzumab).

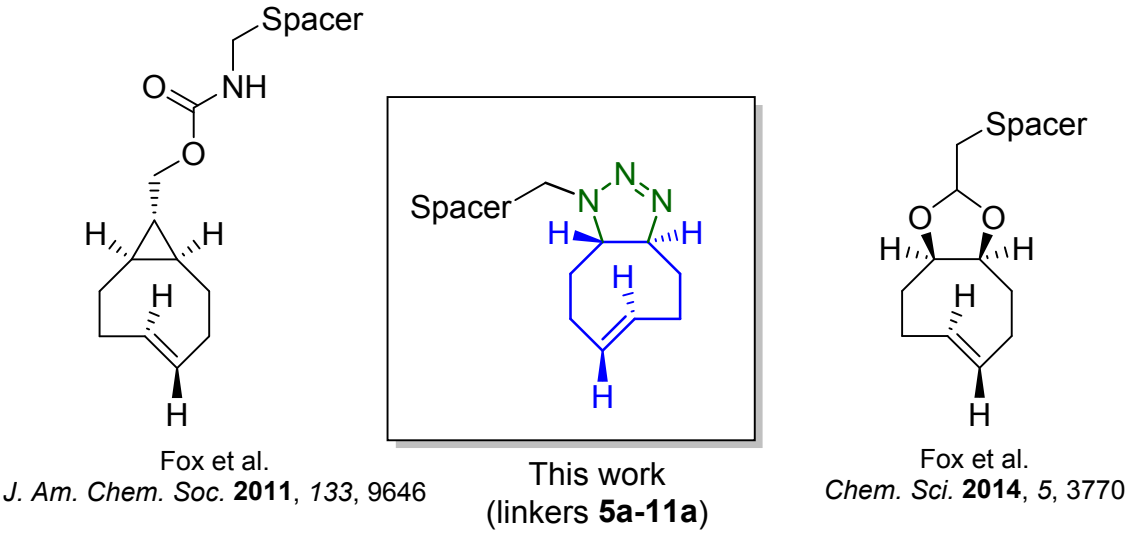

Figure 1. TCO-linkers developed by Fox et al. compared to the novel TCO-linkers **5a-11a** in this manuscript.

RESULTS AND DISCUSSION

Our novel strategy – based on the use of (*E*,*E*)-COD **1** (Scheme 1) as key intermediate – offers innovative possibilities of introducing different types of linkers between the biomolecule and the TCO moiety (step 1, Scheme 1) and tuning the stability and ligation efficiency of the tagged protein, before performing the IEDDA bioorthogonal ligation (step 2, Scheme 1).

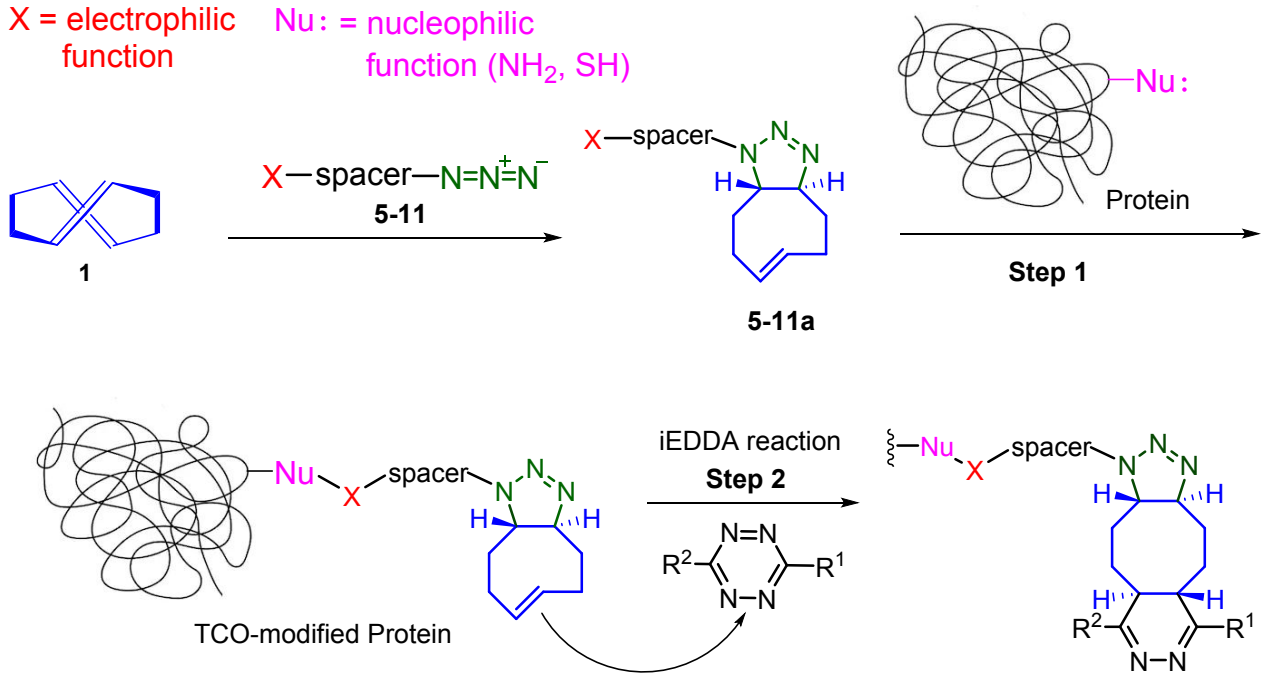

Scheme 1. Schematic representation of the strategy.

Following the experimental procedure reported by Stöckmann et al.,[32] (*E*,*E*)-COD **1** was synthesized through a phosphine-oxide mediated olefin inversion, starting from the cheap starting material (*Z*,*Z*)-COD (the original purification

steps were modified and optimised, as detailed in the Supporting Information). Diolefin **1** is highly volatile and can be stored for months at -20 °C as a solution in hexane or dichloromethane. It can be transferred to other water-immiscible organic solvents by exploiting its complexation with Ag(I). Then, by addition of ammonia, **1** can be extracted back into the desired organic solvent. The concentration of **1** was accurately measured by ^{1}H NMR using glycine as internal standard, allowing careful stoichiometric control in the reaction with the dipolarophile (1.2 equiv).

The high strain energy of (*E*,*E*)-COD **1** triggers a first rapid strain-promoted [3+2] cycloaddition with azides, as reported by Stöckmann et al.[32] Then, the second *trans* olefinic bond of the resulting 1,2,3-triazoles can be subject to an efficient IEDDA reaction with electron-poor tetrazines.[32] Although the rate constant for the IEDDA reaction between benzyl azide monoadduct of **1** and dipyridyl-tetrazine (k_2 = 297±27 $M^{-1}s^{-1}$ in MeOH)[32] is slower than that observed with conformationally-strained TCO derivatives (k_2 = 22,000±2,000 $M^{-1}s^{-1}$ in CD_3OD for cyclopropane-fused TCO-derivatives, see Fig. 1),[26,27] it is still in the expected range for this type of reactions.[6] Even faster rates can be achieved by performing IEDDA reactions in aqueous medium rather than in organic phase, due to the hydrophobic effect.[8] Initially, as a proof of concept study, we decided to test the reactivity of (*E*,*E*)-COD **1** with three model 1,3-dipoles – two azides (**2**, **3**) and a nitrone (**4**) – which afforded, respectively, monoadducts **2a**, **3a** and diastereomeric mixture **4a/b** in excellent yields (Scheme 2). Next, the stability of triazoline-fused TCO derivatives **2a** and **3a** was tested in a protic solvent such as CD_3OD (70 and 35 mM, respectively) over 2 days at room temperature *via* NMR. Both compounds were substantially stable for several hours, but the formation of by-products became evident after 6 hours (see Fig. S5 and S6, Supporting Information, for further details).

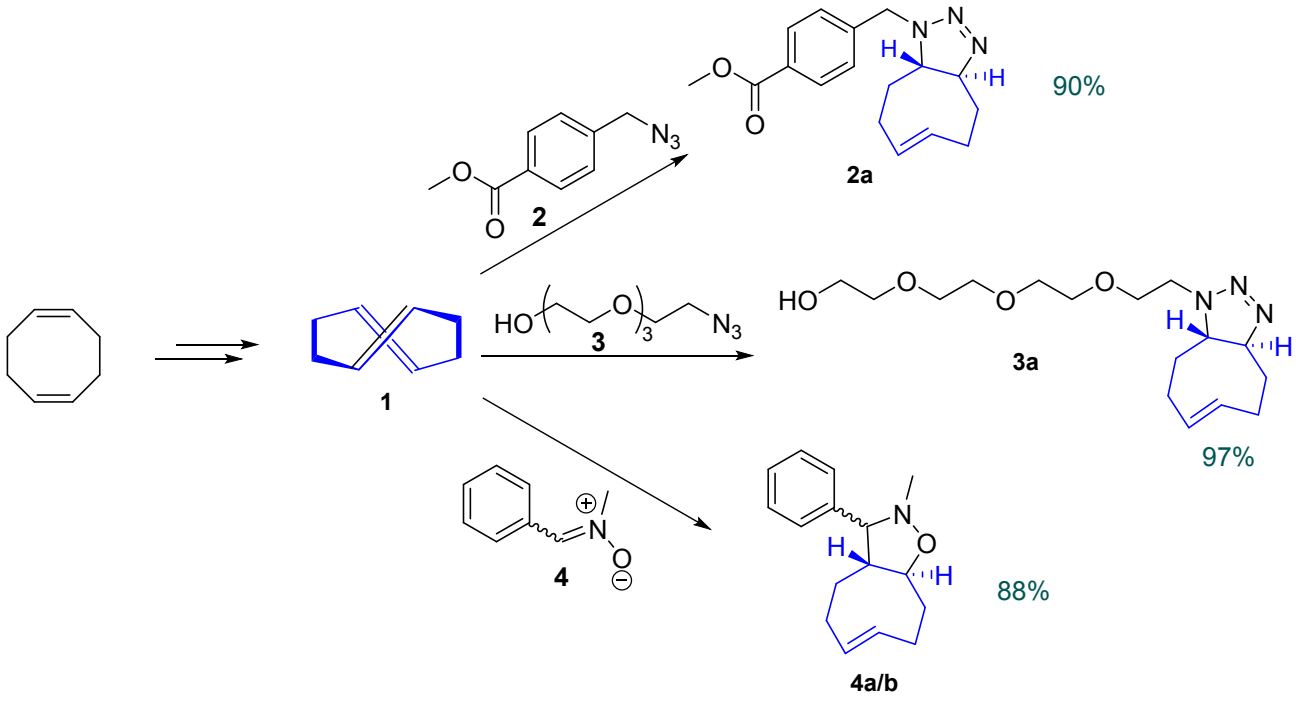

Scheme 2. Test synthesis of three different bicyclic TCO derivatives.

Next, several electrophilic cross linkers carrying a terminal azide function (**5-11**) were synthesized and subsequently reacted with (*E*,*E*)-COD (**1**) to form *trans*-1,2,3-triazoline-fused *trans*-cyclooctene linkers **5a-11a** (Scheme 3). The [3+2] cycloadditions proceeded in approximatively 2 hours at room temperature and the excess of **1** was simply removed by rotary evaporation providing triazolines **5a**-**11a** in nearly quantitative yields. The spacers spanned from a hydrophobic and rigid *p*-methylbenzoate (**6a** and **7a**) to a less hydrophobic acetate (**5a**) and hydrophilic/flexible short PEG chains (**8a**-**11a**). Among the PEGylated triazoline-TCO linkers, succinimidyl carbonate derivative **9a** was found to be exceedingly reactive, releasing *N*-hydroxysuccinimide even in the presence of traces of moisture present in an organic

solvent, such as CD_2Cl_2. On the other hand, *para*-nitrophenyl carbonate **10a** demonstrated a lower reactivity, in line with previous reports.[33] Succinimidyl ester **8a** represents a compromise in terms of reactivity/stability between the previous two. Regarding maleimide-azide cross-linkers **7** and **11**, we observed limited stability upon storage even at 4 °C, due to the azido group being prone to undergo 1,3-dipolar cycloaddition with the maleimide double bond, forming mixtures of the corresponding 1,2,3-triazoles.[34,35] Therefore, these linkers had to be freshly synthesized, avoiding their purification on silica gel (especially for linker **11**), and used immediately in the click reaction with (*E*,*E*)-COD **1**.

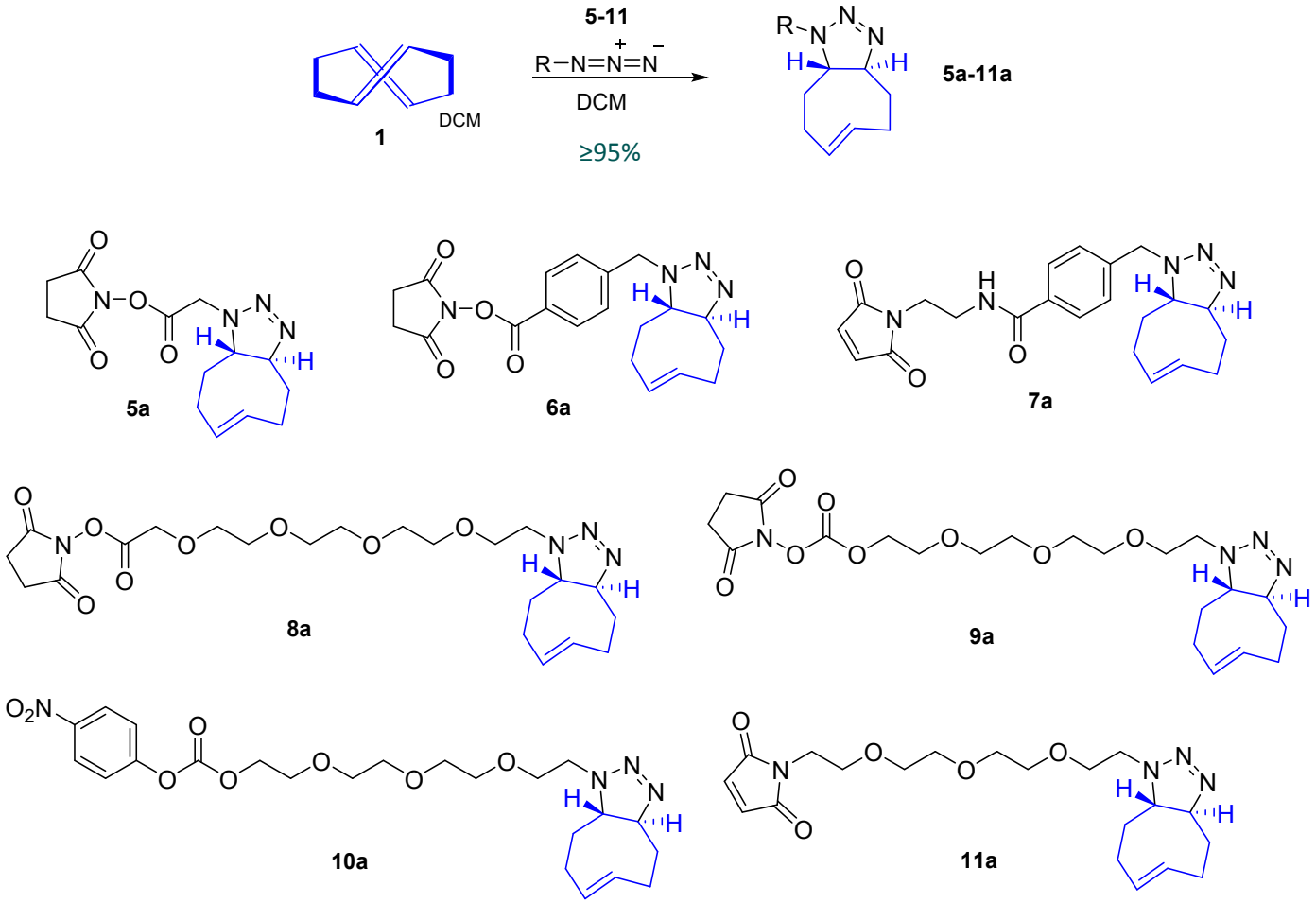

Scheme 3. General method for the synthesis of triazolines **5a**-**11a**.

With these novel TCO linkers (**5a**-**11a)** in hand, we conducted different bioconjugation studies to evaluate their potential as bioorthogonal chemical reporters. We selected TCO derivative **8a** for testing the coupling with the free lysine residues of BSA, because of its favourable overall reactivity/stability properties (see above). TCO-modified BSA was obtained by treatment of BSA with **8a** and subsequently incubated with different concentrations of fluorescein isothiocyanate (FITC)-tetrazine **12**, which was synthesized by coupling of methyl-tetrazine-amine (**13**) with commercially available FITC isomer I (**14**) (Scheme 4). The resulting fluorescent product was then assayed by SDS-PAGE and in-gel fluorescent measurement, showing that fluorescein labelling of TCO-modified BSA proceeded efficiently in a dose-dependent manner with some background labelling of unmodified BSA at higher concentrations of tetrazine **12** (Fig. 2A).

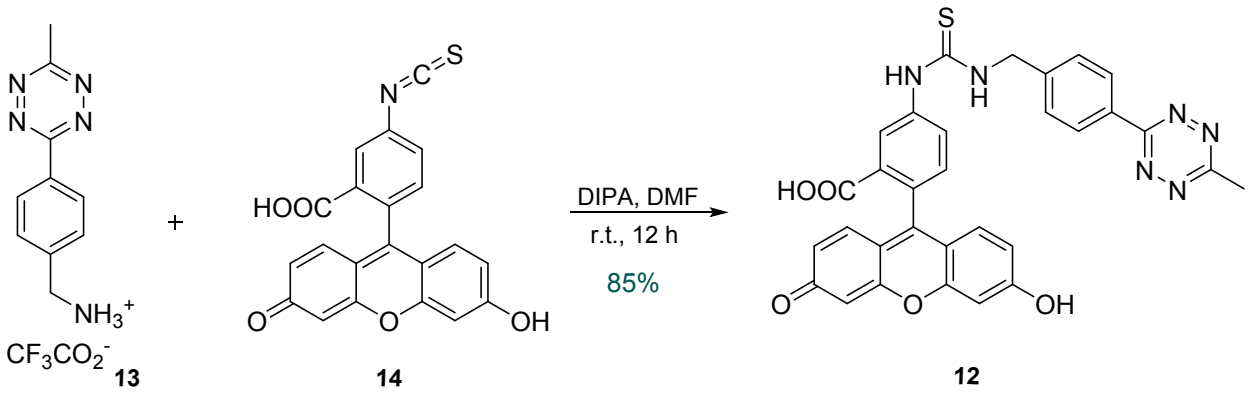

13 **14** **12**

Scheme 4. Synthesis of FITC-tetrazine **12**.

To assess if the TCO/tetrazine ligation was specific, just 5% of **8a**-modified BSA was added to a cellular lysate and incubated with FITC-tetrazine **12**, which resulted in a single fluorescent band, corresponding to 70 kDa (BSA), confirming the bioorthogonality of the reaction, even in presence of a complex mixture of proteins. This result also confirmed the ability of the reaction to occur within minutes at low biomolecule concentrations, which is an important feature for bioorthogonal reactions.

Encouraged by these results, the utility of our novel *trans*-cyclooctene linkers for live-cell imaging was investigated next (Fig. 2B,C). As proof of principle in a biological system, the potential of the water-soluble PEG-TCO-linker **8a** for labelling a bacterial pathogen, *S. aureus*, *via* ligation of the free amino groups of peptidoglycan on the bacterial wall was assessed. Then, modified and unmodified bacteria, both expressing green fluorescent protein (GFP), were incubated with 6-methyl-tetrazine-sulfo-Cy3 (Tz-sulfo-Cy3). Only the peptidoglycan of bacteria treated with **8a** showed bright fluorescence in the red channel, as a consequence of successful binding to Tz-sulfo-Cy3. This result was confirmed by FACS analysis of labelled and unlabelled bacteria (Fig. 2C). Finally, the cytotoxicity of the treatment was examined confirming that neither the TCO linker nor the tetrazine treatment affected bacterial growth.

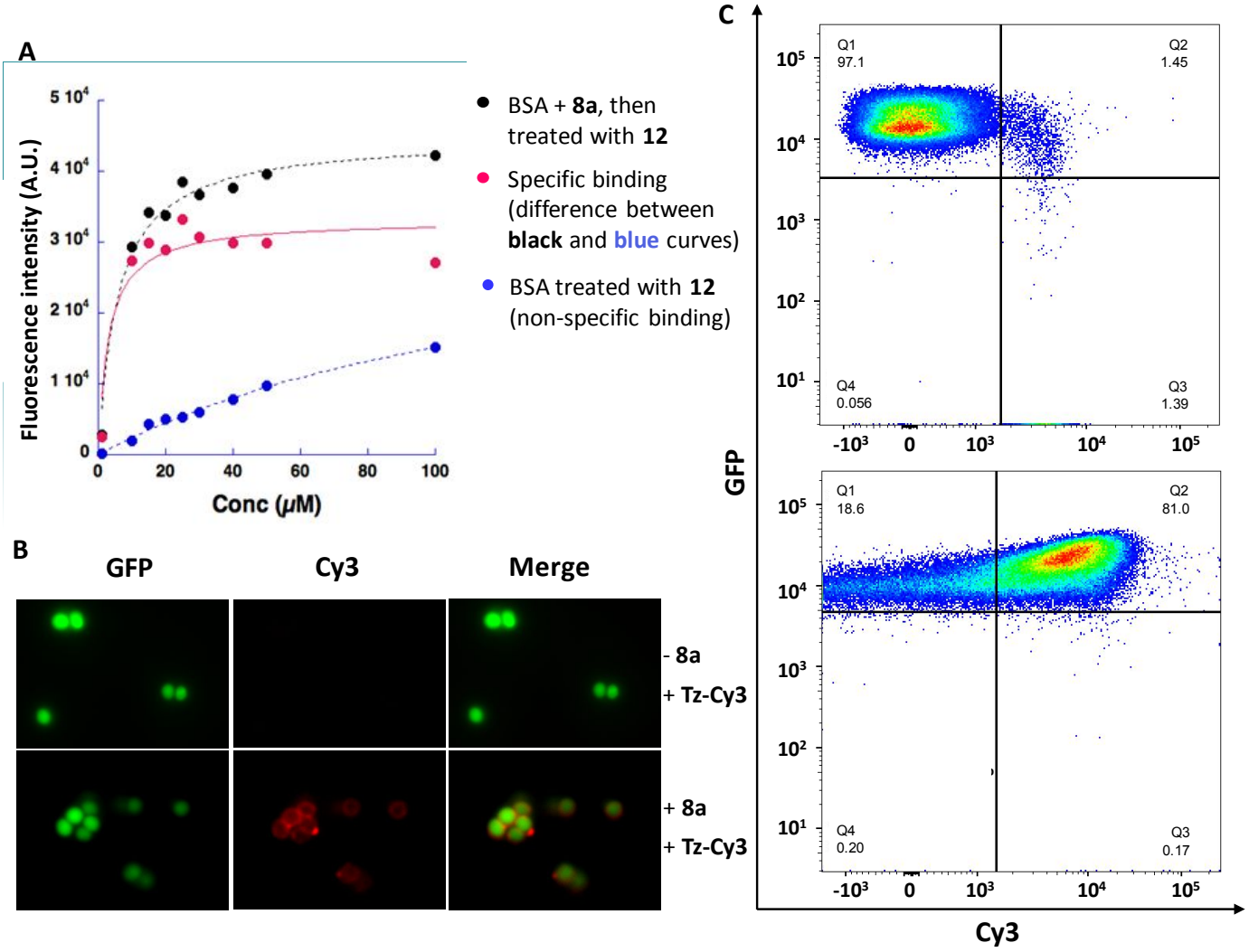

Figure 2. Bioconjugation of BSA (**A**) and gram-positive *S. aureus* bacteria (**B** and **C**) using linker **8a**. (**A**) SDS-PAGE analysis of unlabelled and **8a**-labelled BSA treated with fluorescent tetrazine (Tz) **12** and measurement of specific binding at different probe concentrations: BSA was either incubated with **8a** (black curve) or not incubated (blue curve) and subsequently treated with FITC-tetrazine **12**. Specific binding (pink curve) was calculated by subtracting the non-specific binding BSA fluorescence from BSA+**8a** fluorescence (i.e. black curve minus the blue curve). (**B**) Microscopic analysis of *S. aureus* expressing green fluorescent protein (GFP), showing that bacteria modified with compound **8a** (lower panel) are selectively labelled by Tz-sulfo-Cy3, whereas those not treated with **8a** (upper panel) are not labelled. The green channel (GFP, left) shows all the bacteria, the red channel (Cy3, middle) shows that only the peptidoglycan of *S. aureus* previously treated with **8a** binds Tz-sulfo-Cy3, as confirmed by merging images from GFP and Cy3 channels (right). (**C**) Flow cytometry analysis of unlabelled (upper panel) and **8a**-labelled (lower panel) GFP-expressing *S. aureus*, treated with Tz-sulfo-Cy3: only a minority (1.45%) of non-**8a**-treated bacteria (upper panel) showed detectable level of binding to Tz-sulfo-Cy3, while > 80% of **8a**-treated bacteria showed high Cy3 fluorescence (lower panel).

Next, the three different bicyclic TCO derivatives, *p*-azidomethylbenzoate **6a** and short PEG-linkers **8a** and **10a**, were compared for their capacity to successfully modify therapeutic antibodies. These TCO-linkers were chosen to test the effect of different spacers (with or without PEG, as in **6a** or **8a** and **10a** respectively) and terminal electrophilic functions (NHS or *p*-nitro phenyl carbonate, as in **6a, 8a** or **10a**, respectively). As demonstrated in the literature,[36–38] the linker is a key factor in determining bioorthogonal ligation efficiency with *trans*-cyclooctene conjugated antibodies. It can affect the *in vitro*/*in vivo* TCO stability and reactivity,[36,37] its accessibility on the antibody surface as well as the aqueous solubility[38] of the final construct. Rituximab was treated with one of the TCO-linkers and after purification by gel-filtration, the number of reactive TCOs per antibody was evaluated by reaction with Tz-sulfo-Cy3 and subsequent absorbance measurements at 280 and 553 nm. Linker **6a** failed to provide any construct carrying reactive TCO handles, causing instead antibody precipitation, as a likely result of aggregation. Presumably, the *p*-azidomethylbenzoate linker increases the protein surface hydrophobicity, thus reducing the construct stability in aqueous solution. We next explored whether the introduction of a short PEG spacer could afford a stable construct with a reproducible TCO/mAb ratio (TAR). We

firstly tested succinimidyl linker-TCO **8a**. Although it enabled successful labelling of BSA and *S. aureus* at neutral pH (7.4), it proved to be fast hydrolysing at basic pH (> 8), leading to quite variable TCO/mAb ratios (TAR ranged from 0.1 to 0.6). For this reason, we switched to the *p*-nitro phenyl carbonate activated linker (**10a**), which is less susceptible to hydrolysis. This allowed us to conduct the conjugation at pH 9.5, to promote the reaction between the nucleophilic amine and the aromatic carbonate group. Linker **10a** provided a reproducible TAR of 0.9 ± 0.0 (*n*=4) for Rituximab conjugation (Fig. 3), with more than 94% of mAb recovered after click reaction. Similar TARs were measured for Obinutuzumab conjugation and size-exclusion chromatograms at 280 and 553 nm showed clean final constructs, with no significant aggregates or fragments (Fig. 4, S3). Cy3-linked TCO-Rituximab remained intact for at least seven days in PBS at 24°C. Although some antibody degradation was visible at 280 nm, we observed very little dye release, thus indicating the usefulness of this strategy (see Supporting Information for further details).

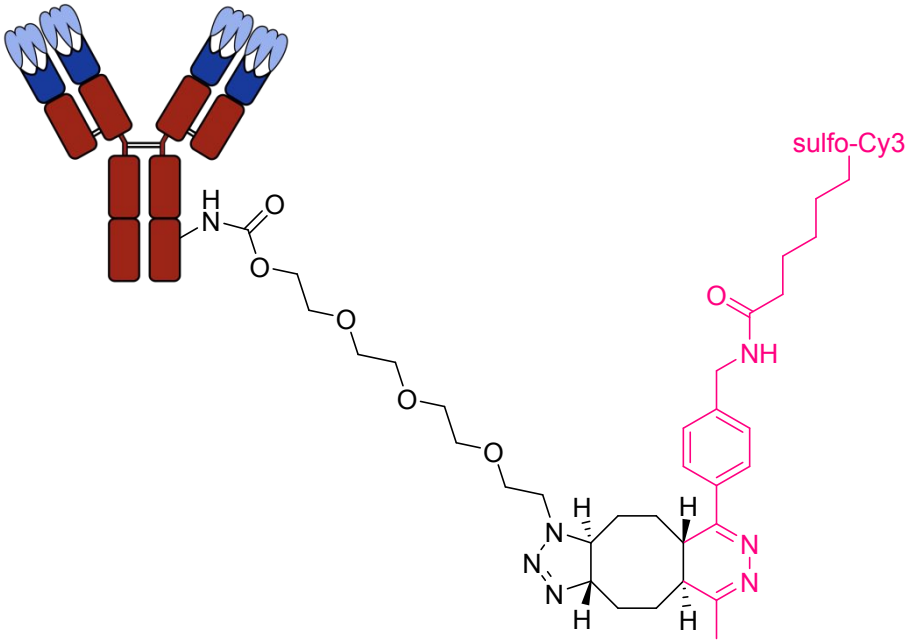

Figure 3. Structure of Tz-sulfo-Cy3-labelled **10a**-Rituximab.

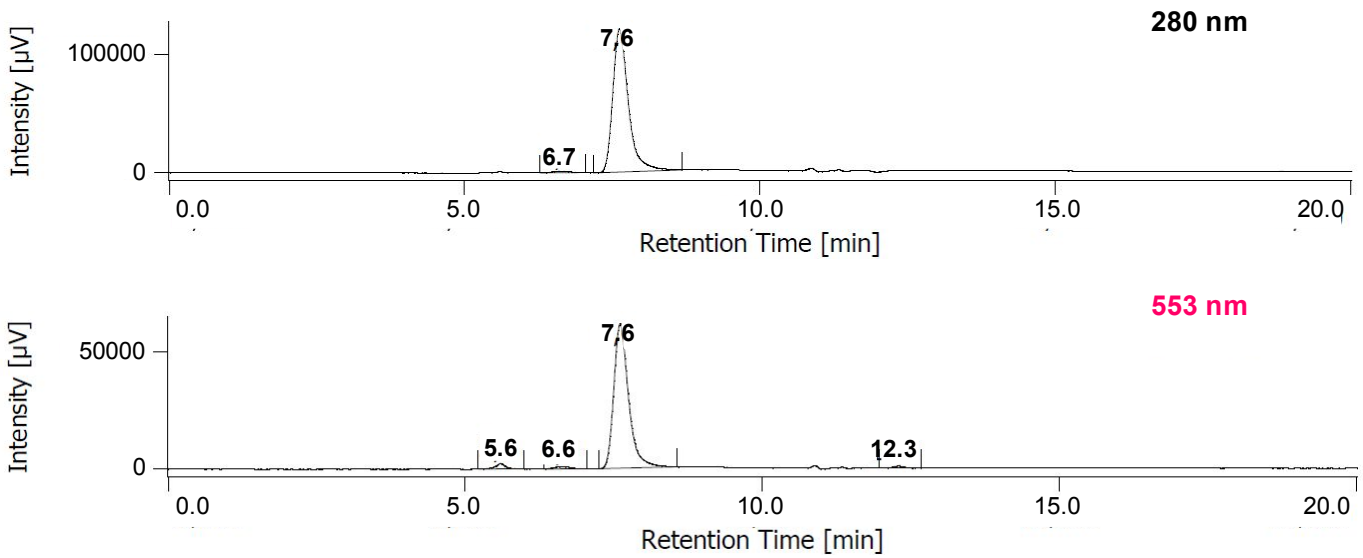

Figure 4. Size-exclusion chromatograms at 280 and 553 nm of Tz-sulfo-Cy3-labelled **10a**-Rituximab (Rt 7.6). The conjugation of Tz-sulfo-Cy3 to **10a**-Rituximab, which absorbs at 280 nm, can be observed by the presence of the peak at 553 nm [maximum absorption of Cy3]. The peak at 553 nm, which originates exclusively from the fluorophore sulfo-Cy3, indicates that **10a**-Rituximab was efficiently conjugated to the fluorescent tag, as a consequence of successful IEDDA reaction between the tetrazine dye and the TCO handle on the antibody.

CONCLUSION

In summary, we synthesized and used novel TCO-linkers **5a-11a** derived from *trans*,*trans*-1,5-cyclooctadiene **1** for the conjugation to different types of biomolecules, which were subsequently subjected to bioorthogonal ligation with tetrazine tags. This strategy offers flexibility in the choice of the linker, which plays an important role on the stability and ligation efficiency of the tagged biomolecule, such as BSA. The novel TCO-linkers proved their usefulness as bioorthogonal ligation reporters. Linker **8a** reacted bioorthogonally in a cellular lysate and enabled the labelling of bacteria, such as *S. aureus*, showing its potential for live-cell imaging. Furthermore, the short PEG linker **10a** could be used for decorating the surface of monoclonal antibodies, such as Rituximab and Obinutuzumab, with functional handles without producing any detectable mAb aggregation or precipitation. In conclusion, these novel linkers represent a versatile and valuable addition to the bioorthogonal ligation toolkit. The use of [(*E*,*E*)-COD] **1** as a precursor significantly expands the structural diversity that can be installed on TCO scaffolds, by taking advantage of the first 'click reaction' leading to TCO-linkers **5-11a**. Furthermore, using inexpensive and readily available [(*Z*,*Z*)-COD] as starting material for preparing **1** offers an economic and laboratory-based alternative to purchasing commercial TCO derivatives, without the need of using specialized equipment, such as UV reactor, pumps and Ag^+-loaded columns.[30] Currently, the only shortcoming of this method is the relatively limited efficiency of the three-step conversion of [(*Z*,*Z*)-COD] into **1**,[32] which could be addressed by developing a more direct and scalable procedure for performing this transformation.

EXPERIMENTAL PROCEDURES

General information. Chemicals were purchased from Sigma-Aldrich unless otherwise specified. 6-methyl-tetrazine sulfo-Cy3 was purchased from Jena Bioscience Ltd. Reactions were monitored by thin-layer chromatography (TLC) on Merck silica gel glass plates (60 F254). Visualisation was accomplished by UV light (254 nm) and/or staining with ceric ammonium molybdate or $KMnO_4$. Flash chromatography was performed using silica gel (60 Å, particle size 40–63 μm) purchased from Merck. ^{1}H NMR and ^{13}C NMR spectra were recorded on a Bruker AVANCE III 400 NMR spectrometer and calibrated using residual non-deuterated solvent as internal reference. Chemical shifts (δ) are reported in parts per million (ppm) and coupling constants (J) are given in Hertz (Hz). When necessary, resonances were assigned using two-dimensional experiments (COSY and HSQC). Specific signals of minor diastereomers in diastereomeric mixtures are indicated by an asterisk. Mass Analyses (MS) were performed using an Agilent 1200 HPLC system coupled to an Agilent G6120 single quadrupole detector equipped with an electrospray ionisation (ESI) source in direct infusion modality. ESI-MS spectra were recorded in positive mode. The tagged antibody was analysed by size-exclusion chromatography using a Jasco HPLC system equipped with a Sepax Zenix-C SEC-300 column (300 Å, 7.8 × 300 mm) and Sepax Zenix-C SEC-300 guard column (Sepax Technologies Inc., Newark, DE, USA) using a mixture of 0.05 mol/L sodium phosphate, 0.15 mol/L sodium chloride (pH 6.8), and 0.01 mol/L NaN_3, as the eluent at a flow rate of 1 mL/minute.

General procedure for the synthesis of triazoline monoadducts (2a-3a, 5a-11a). To (*E*,*E*)-COD (**1**, 1.2 eq., 36 mM in DCM), the appropriate azide (0.05-0.1 mmol, 1.0 eq.) dissolved in DCM (linker **2-10**, 28 mM) or EtOAc (linker **11**) was added while stirring at room temperature. When the reaction had finished (typically 2 h, TLC), the solvent and excess of (*E*,*E*)-COD were removed under reduced pressure. See the separate compounds for follow-up purification strategy.

*Methyl-4-(((3aSR,9aSR,E)-3a,4,5,8,9,9a-hexahydro-1H-cycloocta[d][1,2,3]triazol-1-yl)methyl)benzoate (**2a**).* Flash chromatography (*n*-Hex/EtOAc 8.5:1.5). Crystalline solid (90% yield). R*f* = 0.3 (n-Hex/EtOAc 7:3). ^{1}H NMR (400 MHz, $CDCl_3$) δ: 8.01 (d, *J* = 8.4 Hz, 2H), 7.29 (d, *J* = 8.4 Hz, 2H), 5.46 (ddd, *J* = 15.8, 10.8, 3.4 Hz, 1H), 5.30 (ddd, *J* = 15.8,

10.8, 3.4 Hz, 1H), 4.91 (d, *J* = 15.6 Hz, 1H), 4.52 (d, *J* = 15.6 Hz, 1H), 3.92 (m, 3H), 3.91 (td, *J* = 11.2, 1,6 Hz, 1H), 2.71 – 2.66 (m, 1H), 2.60 (td, *J* = 11.2, 1,6 Hz, 1H), 2.42 – 2.26 (m, 3H), 2.18 – 1.98 (m, 2H), 1.67 – 1.52 (m, 1H), 1.51 – 1.34 (m, 1H). ^{13}C NMR (101 MHz, $CDCl_3$) δ: 166.8, 141.6, 135.7, 134.0, 129.9 (2C), 129.7, 128.3 (2C), 87.2, 65.8, 52.4, 52.2, 37.7, 35.6, 33.3, 32.4. MS (ESI): *m*/*z* calcd $C_{17}H_{21}N_3O_2$: 300.2 $[M+H]^+$; found: 272.1 $[M-N_2+H]^+$, 290.1 $[M-N_2+H_2O+H]^+$.

*2-(2-(2-(2-((3aSR,9aSR,E)-3a,4,5,8,9,9a-Hexahydro-1H-cycloocta[d][1,2,3]triazol-1-yl)ethoxy)ethoxy)ethoxy)ethan-1-ol (**3a**).* Filtration through a pad of silica gel (*n*-Hex/Ac_2O 1:1). Clear oil (97% yield). R*f* = 0.24 (*n*-Hex/Ac_2O 1:1). ^{1}H NMR (400 MHz, D_2O) δ: 5.75 – 5.51 (m, 2H), 4.01 (t, *J* = 11.2 Hz, 1H), 3.91 – 3.55 (m, 16H), 3.23 (t, *J* = 11.2 Hz, 1H), 2.65 – 2.13 (m, 6H), 1.72 (m, 2H). ^{13}C NMR (101 MHz, CD_3OD) δ: 135.1, 134.3, 85.1, 72.3, 70.3, 70.26, 70.2, 70.0, 69.9, 68.7, 66.9, 60.8, 37.3, 35.2, 32.8, 32.0. MS (ESI): *m*/*z* calcd $C_{16}H_{29}N_3O_4$: 328.2 $[M+H]^+$; found: 300.1 $[M-N_2+H]^+$, 318.1 $[M-N_2+H_2O+H]^+$.

*(3RS,3aRS,9aSR,E)-2-Methyl-3-phenyl-2,3,3a,4,5,8,9,9a-octahydrocycloocta[d]isoxazole (**4a/b**).* α-Phenyl-*N*-methylnitrone was synthesized as reported by Bigdeli et al.[39] in 50% yield. In short: nitrone (10 mg, 0.074 mmol, 1.0 eq.) was dissolved in DCM and added to (*E*,*E*)-COD (**1**, 4.8 mL, 20 mM, 1.3 eq.). After 4 h, some nitrone was still present (TLC, DCM/MeOH 9.5:0.5), therefore the reaction was left stirring overnight. The completion of reaction was checked by TLC. The solvent was removed under reduced pressure and the crude product was purified by flash chromatography (100% DCM) to afford 16 mg of diastereomeric mixture (60:40 ratio) of monoadducts (88%). ^{1}H NMR (400 MHz, $CDCl_3$) δ: 7.27 – 7.1 (m, 5H), 5.5 – 5.3 (m, 2H), 3.68 (ddd, *J* = 10.8, 5.2, 1.6 Hz, 1H), 3.45 (d, *J* = 8.8 Hz, 0.6H, H-3), 2.89 (d, *J* = 9.6 Hz, 0.4H, H-3*), 2.44 (s, 1.8H, CH_3), 2.36 (s, 1.2H, CH_3*), 2.34 – 2.06 (m, 5H), 1.83 – 1.72 (m, 2H), 1.41 (m, 1H), 1.15 – 1.10 (m, 1H). ^{13}C NMR (101 MHz, $CDCl_3$) δ: 138.3*, 137.7, 135.5*, 134.3, 133.5, 132.8*, 128.6 (2C), 128.5* (2C), 128.4 (2C), 128.3* (2C), 127.9*, 127.4, 87.9, 86.2*, 80.9*, 77.9, 62.4*, 55.2, 43.4, 43.2*, 40.9*, 37.3, 34.6, 34.1, 34.07*, 33.4*, 32.6*, 31.9. MS (ESI): *m*/*z* calcd $C_{16}H_{21}NO$: 244.2 $[M+H]^+$; found: 244.1 $[M+H]^+$.

*2,5-Dioxopyrrolidin-1-yl-2-((3aSR,9aSR,E)-3a,4,5,8,9,9a-hexahydro-1H-cycloocta[d][1,2,3]triazol-1-yl)acetate (**5a**).* Crystalline solid (quantitative yield). R*f* = 0.2 (*n*-Hex/EtOAc 1:1). ^{1}H NMR (400 MHz, CD_2Cl_2) δ: 5.59 – 5.46 (m, 2H), 4.90 (d, *J* = 17.2 Hz, 1H), 4.36 (d, *J* = 17.2 Hz, 1H), 4.01 (td, *J* = 11.2, 1.6 Hz, 1H), 3.01 (td, *J* = 11.2, 1.6 Hz, 1H), 2.83 (s, 4H), 2.7 – 2.65 (m, 1H), 2.49 – 2.14 (m, 4H), 2.17 – 2.09 (m, 1H), 1.76 – 1.60 (m, 2H). ^{13}C NMR (101 MHz, CD_2Cl_2) δ: 168.8 (2C), 165.1, 135.7, 134.0, 88.9, 65.6, 47.3, 36.9, 35.7, 33.2, 32.2, 25.6 (2C). MS (ESI): *m*/*z* calcd $C_{14}H_{18}N_4O_4$: 307.1 $[M+H]^+$; found: 297.1 $[M-N_2+H_2O+H]^+$.

*2,5-Dioxopyrrolidin-1-yl-4-(((3aSR,9aSR,E)-3a,4,5,8,9,9a-hexahydro-1H-cycloocta[d][1,2,3]triazol-1-yl)methyl)benzoate (**6a**).* Crystalline solid (quantitative yield). R*f* = 0.27 (*n*-Hex/EtOAc 1:1). ^{1}H NMR (400 MHz, CD_3Cl) δ: 8.16 – 8.05 (d, *J* = 8.4 Hz, 2H), 7.37 (d, *J* = 8.4 Hz, 2H), 5.47 (ddd, *J* = 16.1, 10.8, 3.5 Hz, 1H), 5.36 (ddd, *J* = 16.1, 10.8, 3.5 Hz, 1H), 4.92 (d, *J* = 15.7 Hz, 1H), 4.57 (d, *J* = 15.7 Hz, 1H), 3.92 (td, *J* = 11.2, 1.6 Hz, 1H), 2.91 (s, 4H), 2.72 – 2.68 (m, 1H), 2.59 (td, *J* = 11.2, 1.6 Hz, 1H), 2.45 – 2.27 (m, 3H), 2.13 – 2.03 (m, 2H), 1.66 – 1.41 (m, 2H). ^{13}C NMR (101 MHz, CD_3Cl) δ: 169.3 (2C), 161.5, 144.1, 135.8, 133.9, 131.0 (2C), 128.7 (2C), 124.6, 87.4, 65.9, 52.3, 37.6, 35.6, 33.3, 32.3, 25.7 (2C). MS (ESI): *m*/*z* calcd $C_{20}H_{22}N_4O_4$: 383.2 $[M+H]^+$; found: 373.1 $[M-N_2+H_2O+H]^+$.

*N-(2-(2,5-Dioxo-2,5-dihydro-1H-pyrrol-1-yl)ethyl)-4-(((3aSR,9aSR,E)-3a,4,5,8,9,9a-hexahydro-1H-cycloocta[d][1,2,3]triazol-1-yl)methyl)benzamide (**7a**).* Crystalline solid (quantitative yield). R*f* = 0.18 (*n*-Hex/EtOAc 3:7). ^{1}H NMR (400 MHz, CD_3Cl) δ: 7.73 (d, *J* = 8.4 Hz, 2H), 7.27 (d, J = 8.4, 2H), 6.77 (br, 1H, N-H), 6.73 (s, 2H), 5.46 (ddd, *J* = 15.9, 10.8, 3.4 Hz, 1H), 5.31 (ddd, *J* = 15.9, 10.8, 3.4 Hz, 1H), 4.90 (d, *J* = 15.6 Hz, 1H), 4.48 (d, *J* = 15.6 Hz, 1H), 3.90 (td, *J* = 11.2, 1.6 Hz, 1H), 3.84 – 3.81 (m, 2H), 3.67 – 3.63 (m, 2H), 2.69 – 2.65 (m, 1H), 2.61 (td, *J* = 11.2, 1.6 Hz, 1H), 2.43 – 2.26 (m, 3H), 2.12 – 2.02 (m, 2H), 1.66 – 1.54 (m, 1H), 1.48 – 1.38 (m, 1H). ^{13}C NMR (101 MHz, $CDCl_3$) δ: 171.1 (2C),

167.4, 140.1, 135.7, 134.3 (2C), 134.0, 133.6, 128.5 (2C), 127.4 (2C), 87.2, 65.7, 52.2, 39.9, 37.6, 37.5, 35.6, 33.3, 32.4. MS (ESI): *m*/*z* calcd $C_{22}H_{25}N_5O_3$: 408.2 $[M+H]^+$; found: 380.1 $[M-N_2+H]^+$, 398.1 $[M-N_2+H_2O+H]^+$.

*2,5-Dioxopyrrolidin-1-yl-14-((3aSR,9aSR,E)-3a,4,5,8,9,9a-hexahydro-1H-cycloocta[d][1,2,3]triazol-1-yl)-3,6,9,12-tetraoxatetradecanoate (**8a**).* Clear oil (quantitative yield). R*f* = 0.3 (DCM/MeOH 9:1)**.** ^{1}H NMR (400 MHz, $CDCl_3$) δ: 5.59 – 5.36 (m, 2H), 4.50 (s, 2H), 3.84 (td, *J* = 11.2, 1.6 Hz, 1H), 3.78 – 3.76 (m, 2H), 3.72 – 3.46 (m, 14H), 2.98 (td, *J* = 11.2, 1.6 Hz, 1H), 2.83 (s, 4H), 2.71 – 2.66 (m, 1H), 2.48 – 2.29 (m, 3H), 2.24 – 2.14 (m, 2H), 1.71 – 1.52 (m, 2H). ^{13}C NMR (101 MHz, CD_3Cl) δ: 168.8 (2C), 165.9, 135.6, 134.4, 86.6, 71.3, 70.7 (2C), 70.6 (2C), 70.4, 69.5, 67.3, 66.5, 48.0, 37.7, 35.9, 33.4, 32.6, 25.6 (2C). MS (ESI): *m*/*z* calcd $C_{22}H_{34}N_4O_8$: 483.2 $[M+H]^+$; found: 455.1 $[M-N_2+H]^+$.

*2,5-Dioxopyrrolidin-1-yl (2-(2-(2-(2-((3a*SR*,9a*SR*,E)-3a,4,5,8,9,9a-hexahydro-1*H*-cycloocta[*d*][1,2,3]triazol-1-yl)ethoxy)ethoxy)ethoxy)ethyl) carbonate (**9a**).* Clear oil (quantitative yield). R*f* = 0.18 (EtOAc/*n*-Hex 8:2). ^{1}H NMR (400 MHz, CD_2Cl_2) δ: 5.54 – 5.41 (m, 2H), 4.44 – 4.41 (m, 2H), 3.81 (td, *J* = 11.2, 1.6 Hz, 1H), 3.75 – 3.72 (m, 2H), 3.7 – 3.45 (m, 12H), 2.93 (td, *J* = 11.2, 1.6 Hz, 1H), 2.79 (s, 4H), 2.66 – 2.61 (m, 1H), 2.45 – 2.28 (m, 3H), 2.24 – 2.14 (m, 2H), 1.66 – 1.51 (m, 2H). ^{13}C NMR (101 MHz, CD_2Cl_2) δ: 168.7 (2C), 151.6, 135.5, 134.4, 86.8, 70.8, 70.6, 70.5, 70.4, 70.37, 69.2, 68.3, 67.2, 48.2, 37.7, 36.0, 33.3, 32.5, 25.5 (2C). MS (ESI): *m*/*z* calcd $C_{21}H_{32}N_4O_8$: 469.2 $[M+H]^+$; found: 441.2 $[M-N_2+H]^+$, 459.2 $[M-N_2+H_2O+H]^+$.

*2-(2-(2-(2-((3a*SR*,9a*SR*,E)-3a,4,5,8,9,9a-Hexahydro-1*H*-cycloocta[*d*][1,2,3]triazol-1-yl)ethoxy)ethoxy)ethoxy)ethyl (4-nitrophenyl) carbonate (**10a**).* Flash chromatography (*n*-Hex/Ac_2O 7:3). Clear oil (95% yield). R*f* = 0.23 (*n*-Hex/Ac_2O 7:3)**.** ^{1}H NMR (400 MHz, $CDCl_3$) δ 8.30 – 8.25 (d, *J* = 9.2 Hz, 2H), 7.40 – 7.36 (d, *J* = 9.2 Hz, 2H), 5.55 – 5.42 (m, 2H), 4.44 – 4.42 (m, 2H), 3.86 (td, *J* = 11.2, 1.6 Hz, 1H), 3.81 – 3.79 (m, 2H), 3.71 – 3.49 (m, 12H), 2.98 (td, *J* = 11.2, 1.6 Hz, 1H), 2.74 – 2.70 (m, 1H), 2.50 – 2.30 (m, 3H), 2.25 – 2.15 (m, 2H), 1.70 – 1.55 (m, 2H). ^{13}C NMR (101 MHz, $CDCl_3$) δ: 155.5, 152.5, 145.4, 135.6, 134.4, 125.3 (2C), 121.8 (2C), 86.7, 70.74, 70.73, 70.7, 70.4, 69.5, 68.7, 68.3, 67.3, 48.0, 37.8, 35.9, 33.4, 32.6. MS (ESI): *m*/*z* calcd $C_{23}H_{32}N_4O_8$: 493.2 $[M+H]^+$; found: 465.2 $[M-N_2+H]^+$, 483.2 $[M-N_2+H_2O+H]^+$.

*1-(2-(2-(2-(2-((3a*SR*,9a*SR*,E)-3a,4,5,8,9,9a-hexahydro-1*H*-cycloocta[*d*][1,2,3]triazol-1-yl)ethoxy)ethoxy)ethoxy)ethyl)-1*H*-pyrrole-2,5-dione (**11a**).* Filtration through a pad of silica gel (*n*-Hex/EtOAc 2:8). Clear oil (85% yield over two steps). R*f* = 0.2 (EtOAc/*n*-Hex 8:2)**.** ^{1}H NMR (400 MHz, CD_3Cl) δ: 6.69 (s, 2H), 5.55 – 5.42 (m, 2H), 3.86 (td, *J* = 11.2, 1.6 Hz, 1H), 3.74 – 3.48 (m, 16H), 2.99 (td, *J* = 11.2, 1.6 Hz, 1H), 2.74 – 2.69 (m, 1H), 2.51 – 2.31 (m, 3H), 2.26 – 2.16 (m, 2H), 1.70 – 1.54 (m, 2H). ^{13}C NMR (101 MHz, $CDCl_3$) δ: 170.6 (2C), 135.6, 134.4, 134.2 (2C), 86.7, 70.7, 70.6, 70.4, 70.1, 69.5, 67.8, 67.3, 48.0, 37.8, 37.1, 35.9, 33.4, 32.6. MS (ESI): *m*/*z* calcd $C_{20}H_{30}N_4O_5$: 407.2 $[M+H]^+$; found: 379.2 $[M-N_2+H]^+$, 497.2 $[M-N_2+H_2O+H]^+$.

*2-(6-Hydroxy-3-oxo-3H-xanthen-9-yl)-5-(3-(4-(6-methyl-1,2,4,5-tetrazin-3-yl)benzyl)thioureido)benzoic acid (FITC-tetrazine **12**).* (4-(6-Methyl-1,2,4,5-tetrazin-3-yl)phenyl)methanamine (TFA salt) (73 mg, 0.23 mmol, 1.0 eq.) was dissolved in dry DMF (3 mL) under nitrogen atmosphere. Fluorescein-5-isothiocyanate (≥ 90% purity, 105 mg, 0.26 mmol, 1.2 eq.) was added in dry DMF (3 mL), followed by DIPA (65 µL, 0.46 mmol, 2.0 eq.). The reaction was stirred overnight at room temperature (rt). After addition of NH_4Cl (10 mL, sat.aq.), the crude product was extracted in EtOAc (3 x 10 mL). The organic phase was washed with brine (10 mL). The desired product was purified by flash chromatography (gradient from 5% to 15% MeOH in DCM) to yield 112 mg of FITC-tetrazine **12** (yield 85%) as a red solid. R*f* = 0.3 (DCM/MeOH 95/05)**.** ^{1}H NMR (400 MHz, CD_3OD) δ: 8.43 (d, *J* = 8.4 Hz, 2H), 8.13 (m, 1H), 7.74 (dd, *J* = 8.0, 2.0 Hz, 1H), 7.56 (d, *J* = 8.4 Hz, 2H), 7.11 (d, *J* = 8.4 Hz, 1H), 6.63 – 6.59 (m, 4H), 6.47 (dd, *J* = 8.8, 2.4 Hz, 2H), 4.93 (s, 2H), 2.96 (s, 3H). ^{13}C NMR (101 MHz, CD_3OD) δ: 181.9, 169.8, 167.2 (2C), 163.6 (2C), 160.1, 152.8 (2C),

148.1, 143.3, 140.9, 130.7 (2C), 129.0 (2C), 128.9, 128.0 (2C), 127.6 (2C), 124.5, 118.9, 112.4 (2C), 110.1 (2C), 102.2 (2C), 47.5, 19.8. MS (ESI): m/z calcd $C_{32}H_{24}N_6O_4S$: 591,1 $[M+H]^+$; found: 591,1 $[M+H]^+$.

BSA labelling. Bovine serum albumin (BSA) conjugate were prepared by the treatment of BSA (5 mg/mL) with compound **8a** (190 µL of 4 mM, 10 eq.) in PBS (pH 7.4) for 2 hours and subsequent purification by spin-filter (Vivaspin 6, 50 kDa) using PBS (pH 7.4) as buffer.

In-gel fluorescence analysis of BSA conjugates. TCO-modified BSA (1.8 mg/mL) and unmodified BSA (1.8 mg/mL) were diluted (1:2) in PBS (pH 7.4) and treated with FITC-tetrazine **12** (1-100 µM) for 30 minutes at room temperature. Alternatively, 5% of TCO-modified BSA (1.8 mg/mL) was added to total cell lysed from Hela cells (1 mg/mL) and incubated with 15 µL FITC-tetrazine **12** (60 µM) for 5 or 30 minutes. 10 µL of sample buffer 2X (4% SDS, 20% glycerol, 125 mM Tris pH 6.8, 10% β-mercapto-ethanol, 0.001% Bromophenol blue) were added to 10 µL of each BSA sample. The samples were heated for 5 minutes at 99°C and analysed by gel electrophoresis using 10% polyacrylamide gels and running buffer 10X (25 mM Tris base, 192 mM glycine, 3.5 mM SDS, 1 L MilliQ water) diluted (1:10) in MilliQ water. Gel pictures were taken with a UV transilluminator camera and quantified with ImageJ software. Total protein loading was confirmed by subsequent staining with Coomassie Brilliant Blue. Specific binding at each probe concentrations was calculated by subtracting the non-specific binding BSA fluorescence from BSA+**8a** fluorescence.

Bacterial cell culture and labelling experiments. Bacterial cells (*Staphylococcus aureus* SH1000-GFP) from a single colony were grown overnight in LB broth at 37 °C with agitation. An aliquot was taken and diluted (1:100) in fresh broth and cultured for another ~ 2 hours to ensure the bacteria were in the logarithmic phase. Then, 2 aliquots of 1 mL (at a bacterial concentration of a million microliter) were spun down at 3000 g and suspended in 0.5 mL PBS (pH 7.4) or 0.5 mL of compound **8a** in PBS (1 mg/mL, pH 7.4) for 1 h 30 min. The aliquots were spun down at 3000 g, washed twice with 0.5 mL PBS (pH 7.4), spun down again and the bacterial pellet was suspended in 0.5 mL PBS (pH 7.4), followed by incubation with 2 µL of 6-methyl-tetrazine-sulfo-Cy3 (5.5 mM stock solution) at room temperature for 10 min. The bacteria were then sp down and washed twice with 0.5 mL PBS (pH 7.4) before the final dilution of the bacteria in PBS (pH 7.4) for microscopic analysis.

Microscopic analysis of stained cells. For epi-fluorescence microscopy, 10 µL of the bacterial cell suspension was placed on a glass slide. A coverslip was pressed down on the cell droplet to give a single layer of cells on the glass slides. White light and fluorescence images were taken on a microscope (Zeiss Imager M2) equipped with a filter cube suitable for detection of GFP and Cy3 fluorescence. A Plan-NeoFluar × 100 oil lenses from Zeiss was used to visualise the bacterial cells. All images were captured with the exposure time of 150 ms (green fluorescence) or 1600 ms (red fluorescence).

Flow cytometry analysis of stained cells. The samples were prepared and labelled following the same protocol described for microscopy. In addition, cells were resuspended in 4% PFA incubated for 15 minutes at room temperature, then pelleted again, washed once in PBS and then resuspended in PBS (pH 7.4). 300 µL aliquots were filtered through a 35 µm filter (Nalgene) before analysis. The samples were analysed on a BD Fortessa analyser (BD Biosciences). Data analysis was performed with FlowJo.

Antibody modification. 3.0 mg of **Rituximab** (MabThera/Rituxan Roche, 10 mg/mL in solution for injection) was modified with 55 molar equivalents of compound **10a**, added in 3 aliquots after homogeneous mixing (565 µg in 56.5 µL DMSO). The pH was adjusted to 9.5 with 0.1 M sodium carbonate. The reaction was carried out under agitation for 2 h at 24 °C in the dark. Subsequently, the TCO-modified mAb was purified by PD10 (GE Healthcare Life Sciences, NJ, USA), using PBS (pH 7.4) as eluent. The protein concentration was determined by absorbance measurements at 280

nm (NanoDrop®) using a calibration curve of Rituximab. The final concentration of TCO-modified mAb was 1.5 mg/mL in PBS (pH 7.4).

3.0 mg of **Obinutuzumab** (Gazyva/Gazyvaro Roche 25 mg/mL in solution for injection) was buffer exchanged to 0.9% NaCl by PD10 and modified as described above. The final concentration of TCO-modified mAB was 1.3 mg/mL in PBS (pH 7.4).

TAR measurement: An aliquot of TCO-modified mAb (250 µL) was treated with 10 eq. of 6-methyl-tetrazine-sulfo-Cy3 for 1 h at 24 °C. Subsequently, the labelled mAb was purified by PD10, using PBS (pH 7.4) as eluent. The solution was concentrated to 250 µL using an Amicon Ultra-4 (cut-off 10 kDa) centrifugal device. Protein and fluorophore (sulfo-Cy3) concentrations were determined by absorbance measurements respectively at 280 and 553 nm (NanoDrop®). TAR = nmol/mL (sulfo-Cy3)/nmol/mL (mAb).

ASSOCIATED CONTENT

Supporting information

Experimental procedures for the synthesis of heterobifunctional TCO-linkers **5-11**, SDS-page analyses, stability studies, NMR of compounds **7**, **9**, **11**, **2a-11a**,**12** are supplied as Supporting Information.

AUTHOR INFORMATION

Corresponding author

*E-mail: M.Zanda@lboro.ac.uk

ACKNOWLEDGEMENTS

The authors would like to thank Irene Feiner, Marion van Leeuwen-Chomet and Joey Muns for their helpful insight. We acknowledge financial support from the University of Aberdeen and European Union's Horizon 2020 research and innovation programme under the Marie Skłodowska-Curie grant agreement No 675417.

ABBREVIATIONS

BSA, Bovine serum albumin; IEDDA, inverse-electron-demand Diels-Alder; *S. aureus*, *Staphylococcus aureus*; GFP, green-fluorescent protein; TCO, *trans*-cyclooctene; COD, cyclooctadiene; PEG, polyethylene glycol; NHS, *N*-hydroxysuccinimide; PBS, phosphate buffered saline; FACS, fluorescence-activated cell sorting; Tz, tetrazine; Cy3, cyanine dye.

REFERENCES

(1) Bucci, R., Sloan N.L., Topping L., Zanda M. Highly Strained Unsaturated Carbocycles. *Eur. J. Org. Chem.* 10.1002/ejoc.202000512.

(2) Saxon, E., Bertozzi, C. R. (2000) Cell Surface Engineering by a Modified Staudinger Reaction. Science 287, 2007–2010.

(3) Patterson, D. M., Nazarova, L. A., Prescher, J. A. (2014) Finding the Right (Bioorthogonal) Chemistry. ACS Chem. Biol. 9, 592–605.

(4) Carboni, R. A., Lindsey Jr, R. V. (1959) Reactions of Tetrazines with Unsaturated Compounds. A New Synthesis of Pyridazines. J. Am. Chem. Soc. 81, 4342–4346.

(5) Thalhammer F., Wallfahrer U., Sauer J. (1990) Reaktivität einfacher offenkettiger und cyclischer dienophile bei Diels-Alder-reaktionen mit inversem elektronenbedarf. Tetrahedron Lett. 31, 6851–6854.

(6) Blackman, M. L., Royzen, M., Fox, J. M. (2008) Tetrazine Ligation: Fast Bioconjugation Based on Inverse-Electron-Demand Diels−Alder Reactivity. J. Am. Chem. Soc. 130, 13518–13519.

(7) Devaraj, N. K., Weissleder, R., Hilderbrand, S. A. (2008) Tetrazine-Based Cycloadditions: Application to Pretargeted Live Cell Imaging. Bioconjug. Chem. 19, 2297–2299.

(8) Knall, A.-C., Slugovc, C. (2013) Inverse Electron Demand Diels–Alder (IEDDA)-Initiated Conjugation: A (High) Potential Click Chemistry Scheme. Chem. Soc. Rev. 42, 5131–5142.

(9) Serfling, R., Lorenz, C., Etzel, M., Schicht, G., Coin, I. (2018) Designer tRNAs for Efficient Incorporation of Non-Canonical Amino Acids by the Pyrrolysine System in Mammalian Cells. Nucleic Acids Res. 46, 1–10.

(10) Peng, T., Hang, H. C. (2016) Site-Specific Bioorthogonal Labeling for Fluorescence Imaging of Intracellular Proteins in Living Cells. J. Am. Chem. Soc. 138, 14423–14433.

(11) Devaraj, N. K., Upadhyay, R., Haun, J. B., Hilderbrand, S. A., Weissleder, R. (2009) Fast and Sensitive Pretargeted Labeling of Cancer Cells through a Tetrazine/*Trans*-Cyclooctene Cycloaddition. Angew. Chem. Int. Ed. 48, 7013–7016.

(12) Lang, K., Davis, L., Wallace, S., Mahesh, M., Cox, D. J., Blackman, M. L., Fox, J. M., Chin, J. W. (2012) Genetic Encoding of Bicyclononynes and *Trans*-Cyclooctenes for Site-Specific Protein Labeling *in Vitro* and in Live Mammalian Cells via Rapid Fluorogenic Diels–Alder Reactions. J. Am. Chem. Soc. 134, 10317–10320.

(13) Liu, D. S., Tangpeerachaikul, A., Selvaraj, R., Taylor, M. T., Fox, J. M., Ting, A. Y. (2012) Diels–Alder Cycloaddition for Fluorophore Targeting to Specific Proteins inside Living Cells. J. Am. Chem. Soc. 134, 792–795.

(14) Meyer, J.-P., Adumeau, P., Lewis, J. S., Zeglis, B. M. (2016) Click Chemistry and Radiochemistry: The First 10 Years. Bioconjug. Chem. 27, 2791–2807.

(15) Li, Z., Cai, H., Hassink, M., Blackman, M. L., Brown, R. C. D., Conti, P. S., Fox, J. M. (2010) Tetrazine–*Trans*-Cyclooctene Ligation for the Rapid Construction of ^{18}F-Labeled Probes. Chem. Commun. 46, 8043–8045.

(16) Rashidian, M., Keliher, E. J., Dougan, M., Juras, P. K., Cavallari, M., Wojtkiewicz, G. R., Jacobsen, J. T., Edens, J. G., Tas, J. M. J., Victora, G., [et al.] (2015) Use of ^{18}F-2-Fluorodeoxyglucose to Label Antibody Fragments for Immuno-Positron Emission Tomography of Pancreatic Cancer. ACS Cent. Sci. 1, 142–147.

(17) Wu, Z., Liu, S., Hassink, M., Nair, I., Park, R., Li, L., Todorov, I., Fox, J. M., Li, Z., Shively, J. E., [et al.] (2013) Development and Evaluation of ^{18}F-TTCO-Cys40-Exendin-4: A PET Probe for Imaging Transplanted Islets. J. Nucl. Med. 54, 244–251.

(18) Oliveira, B. L., Guo, Z., Bernardes, G. J. L. (2017) Inverse Electron Demand Diels–Alder Reactions in Chemical Biology. Chem. Soc. Rev. 46, 4895–4950.

(19) Zeglis, B. M., Sevak, K. K., Reiner, T., Mohindra, P., Carlin, S. D., Zanzonico, P., Weissleder, R., Lewis, J. S. (2013) A Pretargeted PET Imaging Strategy Based on Bioorthogonal Diels-Alder Click Chemistry. J. Nucl. Med. 54, 1389–1396.

(20) Meyer, J.-P., Houghton, J. L., Kozlowski, P., Abdel-Atti, D., Reiner, T., Pillarsetty, N. V. K., Scholz, W. W., Zeglis, B. M., Lewis, J. S. (2016) ^{18}F-Based Pretargeted PET Imaging Based on Bioorthogonal Diels–Alder Click Chemistry. Bioconjug. Chem. 27, 298–301.

(21) Evans, H. L., Nguyen, Q.-D., Carroll, L. S., Kaliszczak, M., Twyman, F. J., Spivey, A. C., Aboagye, E. O. (2014) A Bioorthogonal ^{68}Ga-Labelling Strategy for Rapid *in Vivo* Imaging. Chem. Commun. 50, 9557–9560.

(22) Rossin, R., Renart Verkerk, P., van den Bosch, S. M., Vulders, R. C. M., Verel, I., Lub, J., Robillard, M. S. (2010) *In Vivo* Chemistry for Pretargeted Tumor Imaging in Live Mice. Angew. Chem. Int. Ed. 49, 3375–3378.

(23) Fang, Y., Judkins, J. C., Boyd, S. J., am Ende, C. W., Rohlfing, K., Huang, Z., Xie, Y., Johnson, D. S., Fox, J. M. (2019) Studies on the Stability and Stabilization of *Trans*-Cyclooctenes through Radical Inhibition and Silver (I) Metal Complexation. Tetrahedron 75, 4307–4317.

(24) Houghton, J. L., Zeglis, B. M., Abdel-Atti, D., Sawada, R., Scholz, W. W., Lewis, J. S. (2016) Pretargeted Immuno-PET of Pancreatic Cancer: Overcoming Circulating Antigen and Internalized Antibody to Reduce Radiation Doses. J. Nucl. Med. 57, 453–459.

(25) Rossin, R., Versteegen, R. M., Wu, J., Khasanov, A., Wessels, H. J., Steenbergen, E. J., ten Hoeve, W., Janssen, H. M., van Onzen, A. H. A. M., Hudson, P. J., [et al.] (2018) Chemically Triggered Drug Release from an Antibody-Drug Conjugate Leads to Potent Antitumour Activity in Mice. Nat. Commun. 9, 1484.

(26) Taylor, M. T., Blackman, M. L., Dmitrenko, O., Fox, J. M. (2011) Design and Synthesis of Highly Reactive Dienophiles for the Tetrazine–*Trans*-Cyclooctene Ligation. J. Am. Chem. Soc. 133, 9646–9649.

(27) Darko, A., Wallace, S., Dmitrenko, O., Machovina, M. M., Mehl, R. A., Chin, J. W., Fox, J. M. (2014) Conformationally Strained *Trans*-Cyclooctene with Improved Stability and Excellent Reactivity in Tetrazine Ligation. Chem. Sci. 5, 3770–3776.

(28) Lambert, W. D., Scinto, S. L., Dmitrenko, O., Boyd, S. J., Magboo, R., Mehl, R. A., Chin, J. W., Fox, J. M., Wallace, S. (2017) Computationally Guided Discovery of a Reactive, Hydrophilic *Trans*-5-Oxocene Dienophile for Bioorthogonal Labeling. Org. Biomol. Chem. 15, 6640–6644.

(29) Kozma, E., Nikić, I., Varga, B. R., Aramburu, I. V., Kang, J. H., Fackler, O. T., Lemke, E. A., Kele, P. (2016) Hydrophilic *Trans*-Cyclooctenylated Noncanonical Amino Acids for Fast Intracellular Protein Labeling. ChemBioChem 17, 1518–1524.

(30) Royzen, M., Yap, G. P. A., Fox, J. M. (2008) A Photochemical Synthesis of Functionalized *Trans*-Cyclooctenes Driven by Metal Complexation. J. Am. Chem. Soc. 130, 3760–3761.

(31) Wittig, G., Polster, R. (1958) ZUM HOFMANN-ABBAU AM CYCLOOCTAN-SYSTEM III. Mitteilung über den modifizierten Hofmann-Abbau. Justus Liebigs Ann. Chem. 612, 102–108.

(32) Stöckmann, H., Neves, A. A., Day, H. A., Stairs, S., Brindle, K. M., Leeper, F. J. (2011) (*E*,*E*)-1,5-Cyclooctadiene: A Small and Fast Click-Chemistry Multitalent. Chem. Commun. 47, 7203–7205.

(33) Roberts, M. J., Bentley, M. D., Harris, J. M. (2012) Chemistry for Peptide and Protein PEGylation. Adv. Drug Deliv. Rev. 64, 116–127.

(34) Huisgen, R., Mäder, H. (1969) Zur Konfiguration Eines Cis-Disubstituierten Azomethin-Ylids. Angew. Chem. 81, 621–623.

(35) de Loera, D., Garcia-Garibay, M. A. (2012) Efficient Aziridine Synthesis in Metastable Crystalline Phases by Photoinduced Denitrogenation of Crystalline Triazolines. Org. Lett. 14, 3874–3877.

(36) Rossin, R., van den Bosch, S. M., ten Hoeve, W., Carvelli, M., Versteegen, R. M., Lub, J., Robillard, M. S. (2013) Highly Reactive *Trans*-Cyclooctene Tags with Improved Stability for Diels–Alder Chemistry in Living Systems. Bioconjug. Chem. 24, 1210–1217.

(37) Rossin, R., van Duijnhoven, S. M. J., Läppchen, T., van den Bosch, S. M., Robillard, M. S. (2014) *Trans*-Cyclooctene Tag with Improved Properties for Tumor Pretargeting with the Diels–Alder Reaction. Mol. Pharm. 11, 3090–3096.

(38) Rahim, M. K., Kota, R., Haun, J. B. (2015) Enhancing Reactivity for Bioorthogonal Pretargeting by Unmasking Antibody-Conjugated *Trans*-Cyclooctenes. Bioconjug. Chem. 26, 352–360.

(39) Bigdeli, M. A., Nikje, M. M. A. (2001) An Efficient and Rapid Chemoselective Synthesis of *Alfa*-Aryl-*N*-Methylnitrones in Dry Media. Monatshefte für Chemie 132, 1547–1549.